catalysts

MDPI

Article

Versatile Sulfathiazole-Functionalized Magnetic Nanoparticles as Catalyst in Oxidation and Alkylation Reactions

Somayeh Ostovar [1], Daily Rodríguez-Padrón [1], Farveh Saberi [1], Alina M. Balu [1] and Rafael Luque [1,2,*]

[1] Department of Organic Chemistry, University of Cordoba Edificio Marie Curie, Ctra Nnal IV-A, Km. 396, E14014 Cordoba, Spain; s.ostovar2266@gmail.com (S.O.); dailydggs@gmail.com (D.R.-P.); farveh.saberilemraski@gmail.com (F.S.); qo2balua@uco.es (A.M.B.)

[2] Scientific Center for Molecular Design and Synthesis of Innovative Compounds for the Medical Industry, Peoples Friendship University of Russia (RUDN University), 6 Miklukho Maklaya Str., 117198 Moscow, Russia

* Correspondence: rafael.luque@uco.es

Received: 20 February 2019; Accepted: 28 March 2019; Published: 9 April 2019;
Corrected: 29 May 2026



Abstract: Catalyst design and surface modifications of magnetic nanoparticles have become attractive strategies in order to optimize catalyzed organic reactions for industrial applications. In this work, silica-coated magnetic nanoparticles with a core-shell type structure were prepared. The obtained material was successfully functionalized with sulfathiazole groups, which can enhance its catalytic features. The material was fully characterized, using a multi-technique approach. The catalytic performance of the as-synthesized material was evaluated in (1) the oxidation of benzyl alcohol to benzaldehyde and (2) the microwave-assisted alkylation of toluene with benzyl chloride. Remarkable conversion and selectivity were obtained for both reactions and a clear improvement of the catalytic properties was observed in comparison with unmodified γ-Fe_2O_3/SiO_2 and γ-Fe_2O_3. Noticeably, the catalyst displayed outstanding magnetic characteristics which facilitated its recovery and reusability.

Keywords: γ-Fe_2O_3; sulfathiazole; maghemite; benzyl alcohol oxidation; alkylations

1. Introduction

The use of recyclable and reusable heterogeneous nanocatalysts for the development of more efficient industrial processes has become a vital need as well as a highly valuable and sustainable option [1,2]. The enhancement of the nanoparticle features for heterogeneous catalysis has crucial importance and, therefore, has attracted the interest of the scientific community in the past years. [3] In particular, magnetic nanocatalysts have emerged as remarkable supports which can be further modified with different functionalities for several catalytic process, having as well good stability, magnetic properties and, consequently, simple magnetic separation from chemical reactions [3,4]. In this regard, iron oxides have received greater attention due to their broad range of applications. Besides their low cost, these materials can be employed as adsorbents [5,6], battery electrodes [7] as well as in biomedicine [8] and in targeted drug delivery [9].

Numerous magnetic core-shell architectures have been developed for use in catalysis [10]. The preparation of multinuclei magnetic iron oxide core embedded by different shells such as a polymer or silica beads has been reported [11]. Specially, silica shells can be modified simply by immobilizing various organic molecules [12]. 2-Sulfanilamidothiazole, also known as sulfathiazole, (STZ) is an efficient organosulfur compound commonly employed as short-acting sulfa-drug and

antimicrobial [13,14]. Nonetheless, the incorporation of such molecule in nanomaterials for catalytic applications has hardly been described in literature.

The scientific community is facing important challenges related to the synthesis of immobilized nanocatalytic systems with advanced features including low preparation cost, high activity, selectivity, stability, efficient recovery and good recyclability. The efficient preparation of such materials and the enhacement of their catalytic properties could have a crucial role for the development of sustainable oxidation processes at an industrial scale. In particular, alcohol oxidations have been involved in most industrial steps for the production of pharmaceuticals, perfumes, dyes, and agrochemicals [15,16]. Low yields and poor selectivity have been the main drawbacks associated with catalytic oxidation reactions. Recently, the selective oxidation of benzyl alcohols to benzaldehyde by using iron oxide-based nanocomposites [17], ionic liquid-modified MIL-100(Fe) [18], developed copper(I)/TEMPO catalysts (TEMPO = 2,2,6,6-tetramethylpiperidinyl-N-oxyl) [19,20], photocatalytic oxidation by homogeneous $CuCl_2$ [21], metal-free systems [22], photoactive VO@g-C_3N_4 [23] and Co oxide nanoparticles [24], among others have been reported.

In addition, aromatic alkylation reactions have been also widely investigated due to their versatility, allowing the preparation of a broad range of compounds as important intermediates, fragrances, agrochemicals and pharmaceuticals. In this study, we reported the preparation and characterization of sulfathiazole-functionalized magnetically separable γ-Fe_2O_3-nanoparticles (MNPs-STZ) and its application for the selective oxidation of benzyl alcohols to the corresponding benzaldehyde derivative, as well as for the alkylation of toluene with benzyl chloride (Scheme 1).

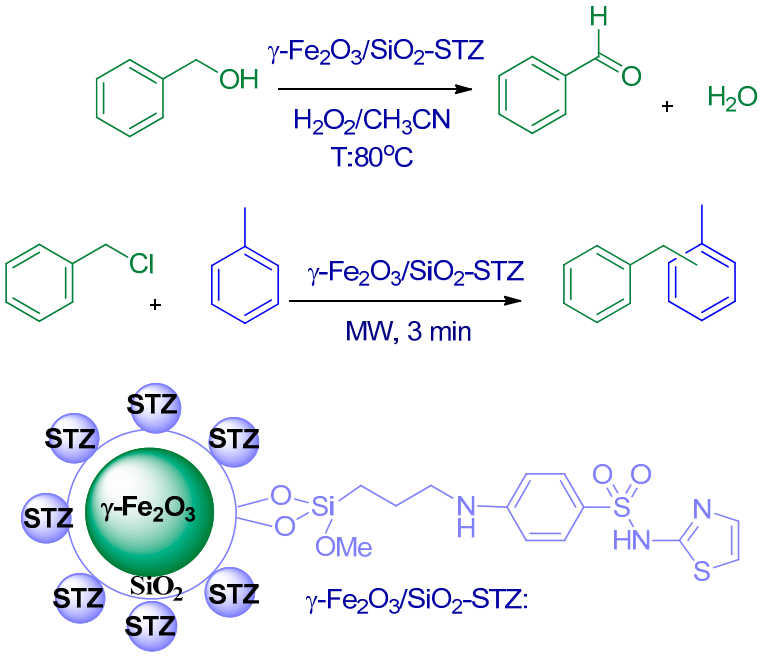

Scheme 1. Oxidation of benzyl alcohol to benzaldehyde and microwave-assisted alkylation of toluene with benzyl chloride by using γ-Fe_2O_3/SiO_2-sulfathiazole (STZ).

2. Results and Discussion

An unprecedented γ-Fe_2O_3/SiO_2-STZ core-shell nanoarchitecture was designed by a multistep strategy involving the covalent attachment of sulfathiazole derivatives on the surface of functionalized γ-Fe_2O_3, as can be observed in Scheme 2. According to the first and second steps, a magnetic phase of iron oxide and a SiO_2 shell have been formed, which will allow, respectively, the simple recyclability of the material and its further modification in order to incorporate in the structure different functionalities with catalytic properties. In a third step, γ-Fe_2O_3/SiO_2 was treated with 3-chloropropylmethoxysilane, consequently giving rise to 3-chloro-propylmethoxysilane-γ-Fe_2O_3/SiO_2

through the formation of covalent bonds. Finally, nucleophilic substitution of chlorine by sulfonamides groups resulted in superparamagnetic γ-Fe_2O_3/SiO_2-STZ nanocatalyst. Such hypothesis was confirmed by a full characterization of the nanomaterial obtained using a multi-technique approach.

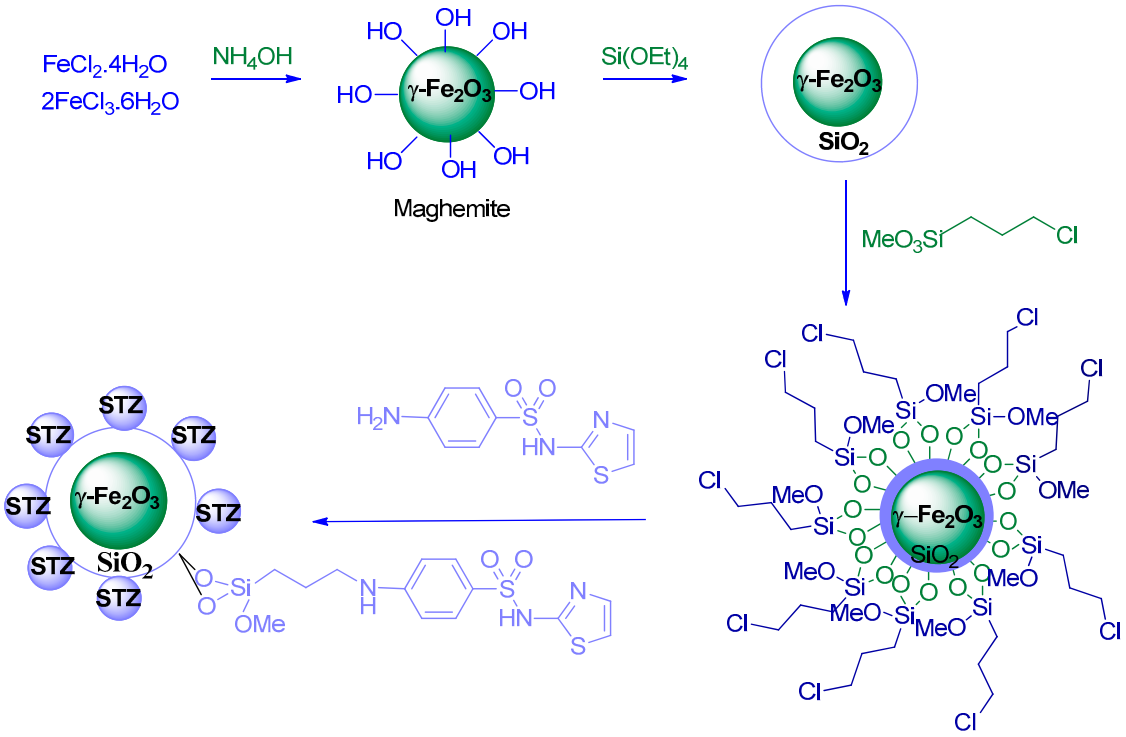

Scheme 2. Multistep strategy for the preparation of γ-Fe_2O_3/SiO_2-STZ.

The morphology of γ-Fe_2O_3/SiO_2-STZ was investigated by scanning electron microscopy (SEM) experiments. No clear evidence was observed for the formation of core-shell structures by SEM analysis (Figure 1A) of γ-Fe_2O_3/SiO_2-STZ, instead a silica-iron oxide composite material appears to be synthesized [12]. As shown in Figure 1A, an SEM image of γ-Fe_2O_3/SiO_2-STZ nanomaterial exhibited a homogeneous distribution of quasi-spherical particle agglomerates with a mean radius of 15 nm (Figure 1C). Elemental composition of the sample was investigated by energy-dispersive X-ray spectroscopy (EDX) analysis, as shown in Figure 1B. Fe, O, C, Si, Cl, N, S were identified by using the aforementioned analysis (Table 1). In particular, the presence of N and S clearly corroborated the successful functionalization of the modified nanoparticles with the STZ group. Nonetheless the peak associated with Cl indicated just a partial nucleophilic substitution of chlorine by sulfonamide.

The crystalline structure of the γ-Fe_2O_3/SiO_2-STZ catalyst was identified by XRD measurements. XRD patterns displayed several diffraction peaks at 30.62°, 35.92°, 43.48°, 54.00°, 57.62° and 63.36°, corresponding to the (220), (311), (400), (422), (511) and (440) crystalline planes of maghemite, respectively (Figure 1C) [25]. This result clearly confirmed the magnetic features of the catalyst core, which will allow its simple recovery and reusability. Through XRD analysis, employing the Williamson–Hall formalism, maghemite crystallite size was also obtained in the range of 9.3–9.4 nm.

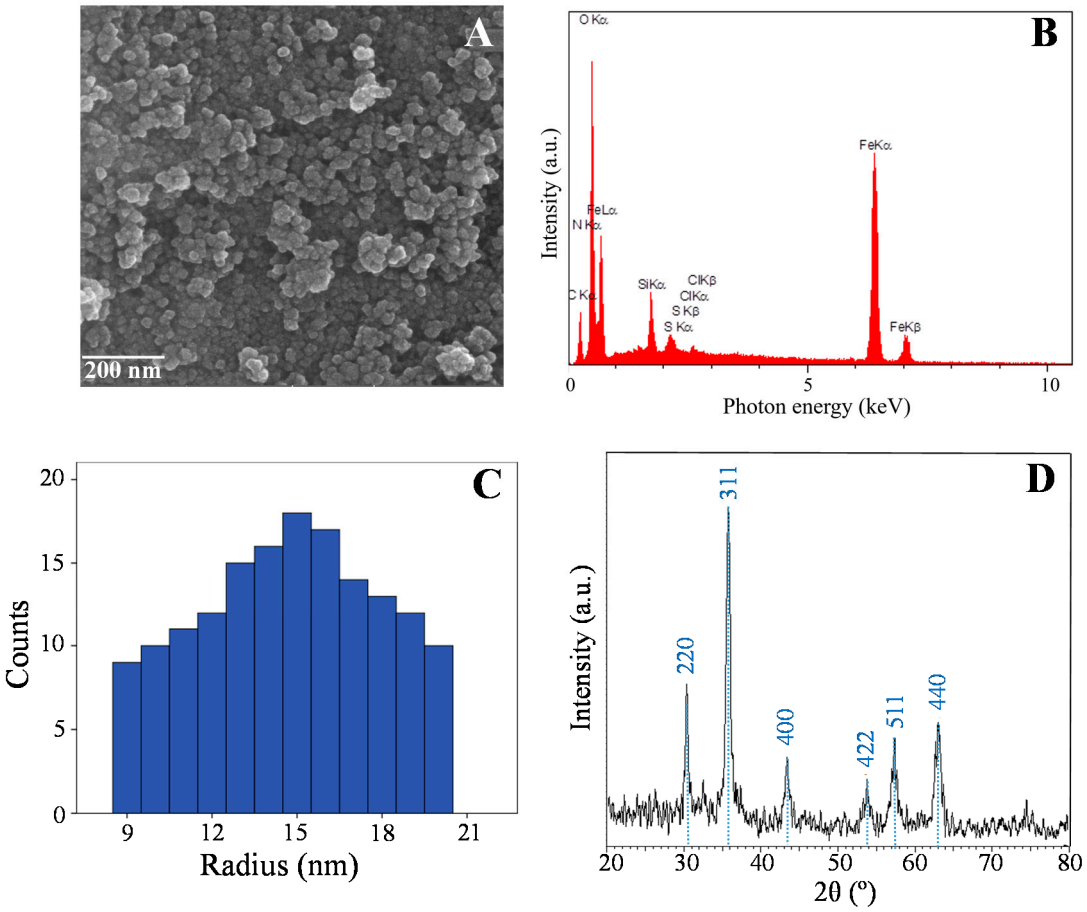

Figure 1. (**A**) Scanning electron microscope (SEM) image, (**B**) energy-dispersive X-ray spectroscopy (EDX) spectrum, (**C**) Particle size distribution and (**D**) X-ray diffraction (XRD) patterns of γ-Fe_2O_3/SiO_2-STZ.

Table 1. Elemental distribution (atomic %) of γ-Fe_2O_3/SiO_2-STZ.

Sample	Fe	O	Si	C	Cl	S	N	Total
γ-Fe_2O_3/SiO_2-STZ	42.1	36.6	1.78	16.88	0.3	0.64	1.65	100

Thermogravimetric analysis further corroborates the presence of supported sulfathiazole in the core-shell γ-Fe_2O_3/SiO_2-STZ. TGA analysis of Fe_2O_3/SiO_2 has been previously reported by our group displaying a negligible weight loss [12]. In turn, a progressive weight loss of 8.6% was observed from 100 °C to 800 °C. Around 200 °C, DTA analysis (Figure 2, green line) displayed a slight endothermic band, related to unbounded/physisorbed solvents [26]. In addition DTA experiments showed two exothermic peaks at 340 °C and 420 °C, associated with the decomposition of sulfathiazole and 3-chloro-propylmethoxysilane, respectively.

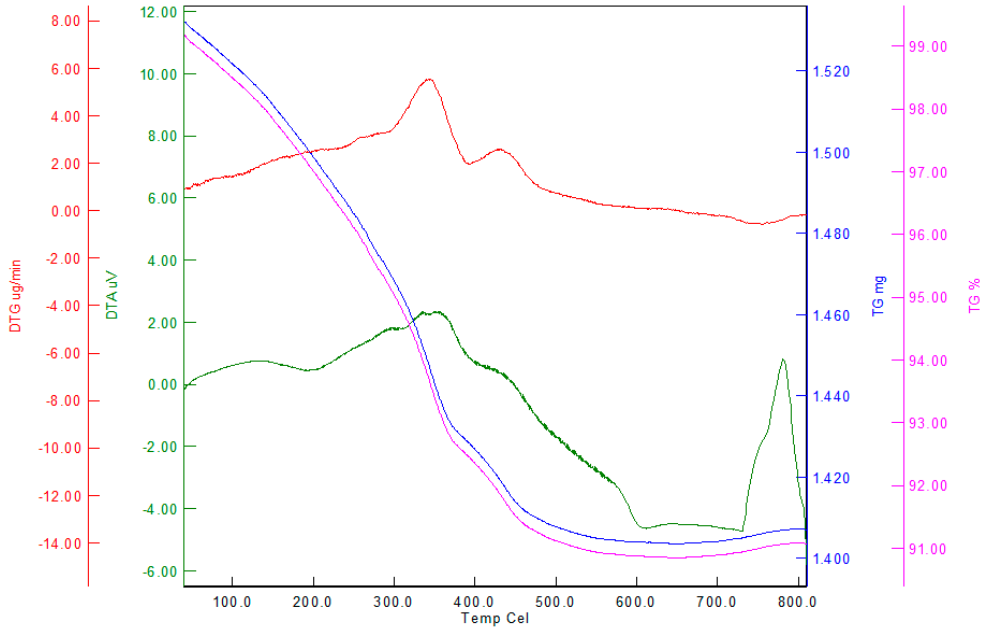

Figure 2. Thermogravimetric and differential thermogravimetric analyses of γ-Fe_2O_3/SiO_2-STZ. Red line: difference thermogravimetry (DTG); green line: difference thermal analysis (DTA); blue line: thermogravimetry analysis (TG) expressed in mg; pink line: TG expressed in wt%.

Fourier transform–infrared (FT–IR) experiments of the obtained materials were performed. Nonetheless, no clear information was obtained from this analysis, most likely due to the low STZ loading in the γ-Fe_2O_3/SiO_2 material (Figure S1). Besides TGA results, STZ successful immobilization was also supported by EDX analysis which revealed the presence of Fe, O, C, Si, Cl, N and S. Particularly, the presence of N and S clearly corroborated the successful functionalization of the modified nanoparticles with the STZ group.

In order to determine the acid properties of the material as well as to distinguish between Lewis and Brønsted acid sites, pyridine (PY) and dimethyl pyridine (DMPY) titration experiments were performed. It was assumed that DMPY selectively titrates Brønsted sites (methyl groups hinder coordination of nitrogen atoms with Lewis acid sites) while PY titrates both Brønsted and Lewis acid sites in the materials. Therefore Lewis acidity was determined as the difference between the amounts of PY (total acidity) and DMPY (Brønsted acidity) adsorbed [27]. The surface acidity of the γ-Fe_2O_3/SiO_2-STZ catalyst resulted in being 265 μmol g^{-1}, with a major contribution of Lewis acid sites (72%, 190 μmol g^{-1}) and a minor percentage of Brϕnsted acidity (28%, 75 μmol g^{-1}).

The magnetic properties of γ-Fe_2O_3/SiO_2-STZ were analyzed by VSM experiments (Figure 3). The saturation magnetization of the prepared nanocore-shell structure was 58.2 emu g^{-1}, corroborating its outstanding magnetic characteristics, which allow its magnetic separation as can be observed in Figure 3, Inset [28].

The catalytic performance of γ-Fe_2O_3/SiO_2-STZ nanocatalyst was investigated in the oxidation of benzyl alcohol to benzaldehyde, employing H_2O_2 as oxidant agent (Table 2). A parametric analysis was performed by analyzing the influence of the catalyst amount and the oxidant agent volume. Figure 4A shows that by increasing the amount of nanocatalyst from 10–25 mg, the conversion increased. Nonetheless, when the catalyst amount increased to 50 mg, no considerable change in conversion was observed, and in turn selectivity values decrease. Therefore, 25 mg was selected as the optimal catalyst amount. Figure 4B reports the catalytic results of the benzyl alcohol oxidation by using different oxidant agent quantities. From 0.1 to 0.2 mL of H_2O_2, an increment of conversion values with negligible change in selectivity was observed. However, by increasing the H_2O_2 volume to 0.5 mL, the selectivity drastically decrease, with the consequent formation of over-oxidation products. Thus, 0.2 mL of H_2O_2 was chosen as optimum value.

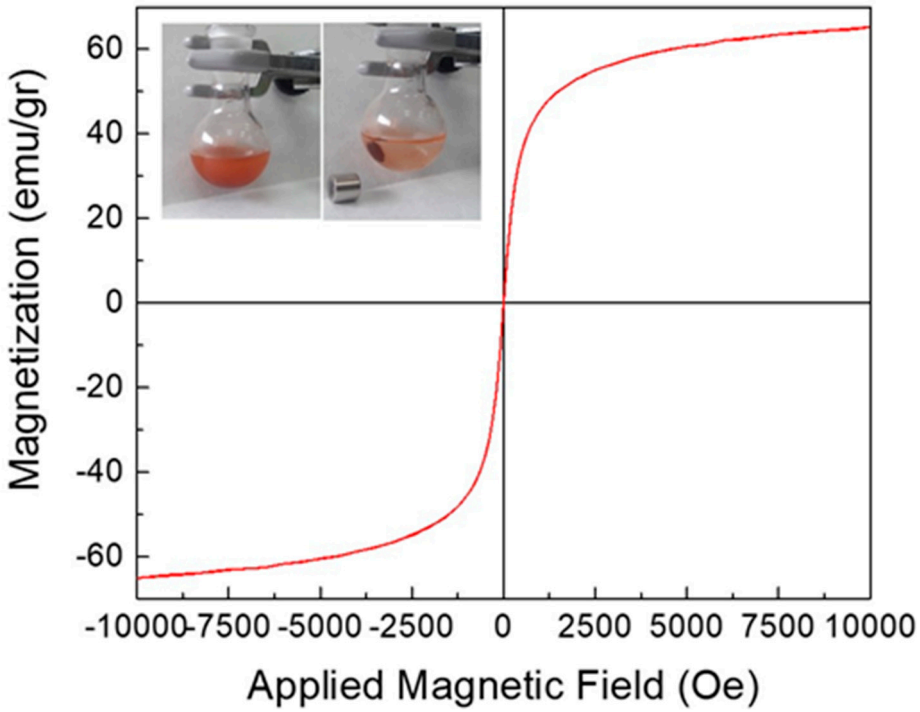

Figure 3. Magnetic curves of γ-Fe_2O_3/SiO_2-STZ. Inset: Left, reaction mixture containing γ-Fe_2O_3/SiO_2-STZ. Right, γ-Fe_2O_3/SiO_2-STZ collected by using an external magnet after the reaction.

Table 2. Results of the oxidation of benzyl alcohol.

Entry	Catalyst	Conversion (mol%)	Selectivity (mol%)
1	Blank (no catalyst)	<10	<10
2	γ-Fe_2O_3	37	>99
3	γ-Fe_2O_3/SiO_2	39	>99
4	γ-Fe_2O_3/SiO_2-STZ	95	97

Reaction condition: benzyl alcohol (1 mmol), H_2O_2 (0.2 mL), catalyst (25 mg), 80 °C, 2 h.

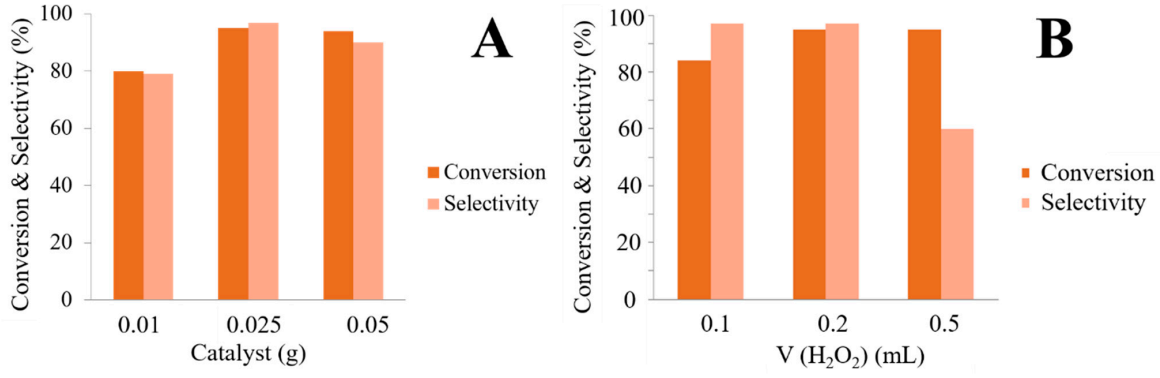

Figure 4. Effect of the reaction parameters on the catalytic performance of γ-Fe_2O_3/SiO_2-STZ (**A**) Catalyst amount, (**B**) H_2O_2 volume (reaction condition: benzyl alcohol (1 mmol), 80 °C, 2 h).

In addition, blank experiments in the absence of catalyst, as well as employing γ-Fe_2O_3/SiO_2 and γ-Fe_2O_3, were accomplished in order to bring out the critical change in the catalytic features after functionalization with sulfathiazole groups. The designed catalytic material (γ-Fe_2O_3/SiO_2-STZ) exhibited remarkable results in terms of conversion (95%) and selectivity (97%), in comparison with

the unmodified γ-Fe_2O_3/SiO_2 γ-and Fe_2O_3, suggesting that sulfathiazole groups endow the magnetic core with outstanding catalytic features.

The designed catalyst was used in the oxidation of several benzyl alcohol derivatives (Table 3), including electron-donating and electron-withdrawing substitution on the aromatic ring, with groups such as $–NO_2$, –Cl, $–CH_3$ or $–OCH_3$. The oxidative conversion of the investigated molecules demonstrated the great versatility of the catalytic system for its application to a broad range of substrates. The proposed mechanism for the benzyl alcohol oxidation is shown in Scheme S1. The oxidation process is based on a surface modification of the active sites by functional sulfathiazole, which decomposes the H_2O_2 to produce hydroxyl radicals and hydroxyl anions [29–31].

Table 3. Catalytic oxidation of different benzyl alcohol derivatives by γ-Fe_2O_3/SiO_2-STZ.

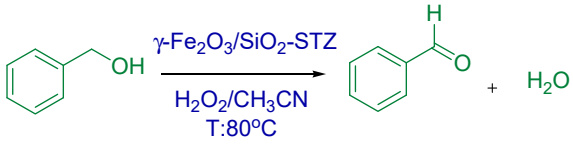

Entry	Substrate	Product	Conversion (mol%)	Selectivity (mol%)
1	benzyl alcohol	benzaldehyde	95	97
2	4-chlorobenzyl alcohol	4-chlorobenzaldehyde	98	96
3	4-methylbenzyl alcohol	4-methylbenzaldehyde	90	95
4	4-methoxybenzyl alcohol	4-methoxybenzaldehyde	97	97
5	4-nitrobenzyl alcohol	4-nitrobenzaldehyde	>99	96

[a] General reaction conditions: a substrate (1 mmol), H_2O_2 (0.2 mL), catalyst (γ-Fe_2O_3/SiO_2-STZ, 25 mg), solvent (acetonitrile, 4 mL), 2 h at 80 °C.

In order to study the stability and reusability of the catalytic material, γ-Fe_2O_3/SiO_2-STZ was recovered, washed with ethanol, and dried at 60 °C. Subsequently, the catalyst was reused in the oxidation of benzyl alcohol and the aforementioned process was repeated 4 times. After the fourth use, the nanocatalyst conserved a good catalytic behavior, obtaining 85% of conversion and 89% of selectivity, as shown in Figure 5.

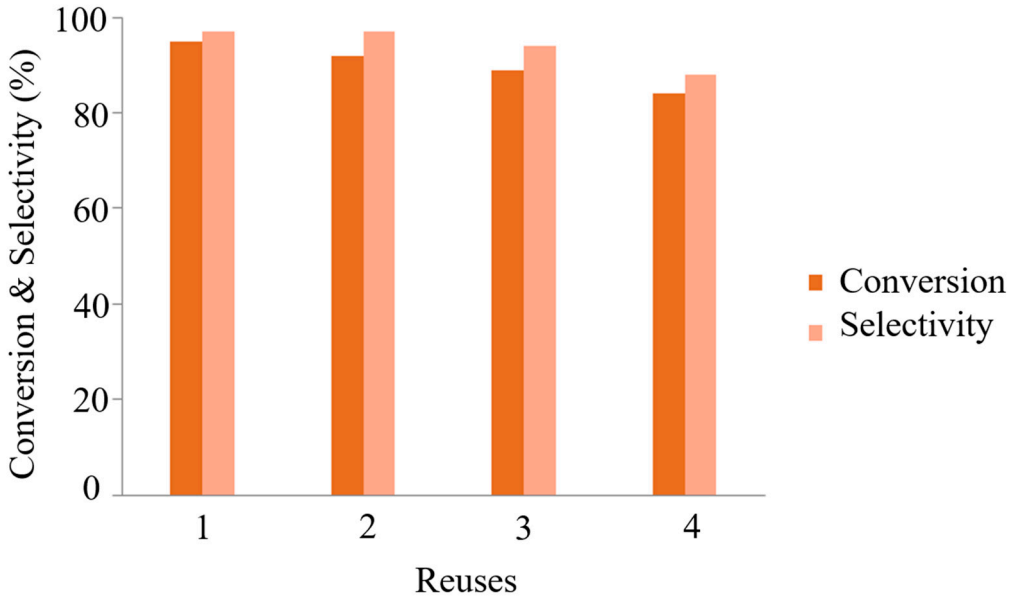

Figure 5. Recycle runs of γ-Fe_2O_3/SiO_2-STZ in the oxidation of benzyl alcohol. Reaction conditions (each run): benzyl alcohol (1 mmol), H_2O_2 (0.2 mL), catalyst (25 mg), 80 °C, 2 h.

In addition to the recycling results, a heterogeneity test was conducted to support the heterogeneous nature of the catalyst. For this purpose, the reaction was carried out under identical reaction conditions

using γ-Fe_2O_3/SiO_2-STZ (1 mmol benzyl alcohol, 0.2 mL hydrogen peroxide, 25 mg catalyst, 4 mL acetonitrile, 80 °C, 1 h) to reach a 55% conversion. The catalyst was then removed using a simple magnet from the reaction mixture and the filtrate (after removal of the catalyst) was left to react for additional 6 h upon the addition of fresh substrate and hydrogen peroxide. The observed conversion after 6 h was 58%, supporting the heterogeneous nature of the reaction since the recovered catalyst (employed in another reaction run) provided >90% conversion at almost complete selectivity to benzaldehyde after 2 h reaction.

Finally, the functionalized composite γ-Fe_2O_3/SiO_2-STZ was tested in the alkylation of toluene with benzyl chloride (Table 4) [32,33]. A proposed mechanism has been included in the supporting information file (Scheme S2). As well, the catalytic activity of γ-Fe_2O_3/SiO_2 and γ-Fe_2O_3 was also investigated. γ-Fe_2O_3/SiO_2-STZ displayed the best catalytic performance with conversion values higher that 99% and a selectivity of 50% to the para-substituted product.

Table 4. Catalytic activity of γ-Fe_2O_3/SiO_2-STZ in the microwave assisted alkylation of toluene with benzyl chloride.

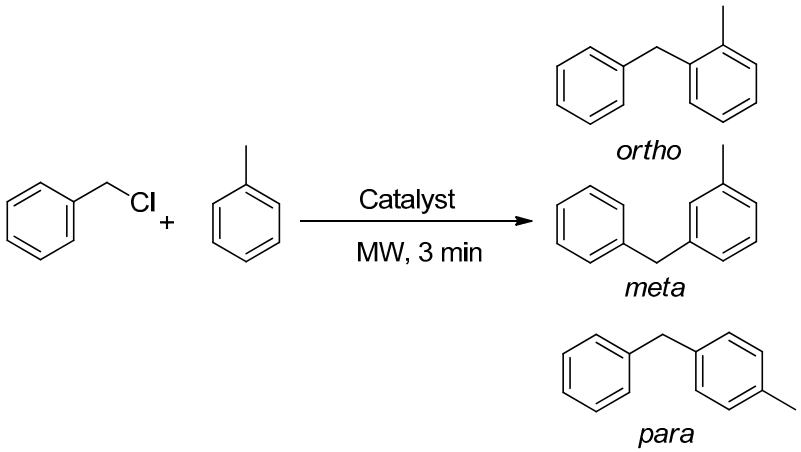

Material	Conversion (mol%)	Selectivity (mol%)		
		Meta	Ortho	Para
γ-Fe_2O_3	70	29	34	37
γ-Fe_2O_3/SiO_2	75	27	33	40
γ-Fe_2O_3/SiO_2-STZ	>99	5	45	50

Reaction conditions: 0.025 g catalyst, 0.2 mL of benzyl chloride, 2 mL of toluene, 300 W (reaction temperature 120 °C).

The results obtained for both reactions are comparable to data reported in the literature. Remarkably, the prepared material displayed an outstanding versatility, resulting to be effective in both alkylation and oxidation reactions. Such versatility is one of the main advantages of the prepared material in comparison with most of the reported materials [34,35].

3. Experimental

3.1. Preparation of γ-Fe_2O_3

Magnetic iron oxide nanomaterial was synthesized according to procedure reported by our group based on a simple coprecipitation methodology [12]. Iron precursors were prepared by dissolving $FeCl_3 \cdot 6H_2O$ (1.09 g) and $FeCl_2 \cdot 4H_2O$ (0.4 g) in a 2 M HCl (4 and 2 mL, respectively) solution. The obtained mixture was vigorously stirred (800 rpm) for 15 min. Subsequently, 50 mL of a 0.7 M NH_4OH solution was slowly added under stirring to the precursor's mixture, in order to achieve a 9–11 pH range. The obtained solid was washed three times with water and ethanol. Finally, the sample was dried at 100 °C for 12 h and further calcined at 300 °C for 3 h.

3.2. Preparation of γ-Fe_2O_3/SiO_2

Maghemite nanoparticles (1 g) were dispersed in ethanol (40 mL) and stirred for 1 h at 40 °C. Subsequently, 5 mL tetraethyl orthosilicate (TEOS) was added to the reaction vessel and the mixture was continuously stirred during 24 h. The silica-coated nanoparticles were collected by an external magnet, washed three times with ethanol and diethyl ether, and finally dried at 100 °C for 12 h under vacuum.

3.3. Preparation of 3-Chloropropyl Trimethoxysilane-γ-Fe_2O_3/SiO_2

1 g of γ-Fe_2O_3@SiO_2 was dispersed in 40 mL of dried toluene by sonication during 45 min. 3-chloropropyl trimethoxysilane (0.5 mL) was added to the dispersed γ-Fe_2O_3@SiO_2 and the mixture was stirred at 105 °C for 24 h. The functionalized γ-Fe_2O_3/SiO_2 was separated by an external magnet, washed three times with diethyl ether and dichloromethane, and dried under vacuum.

3.4. Preparation of γ-Fe_2O_3/SiO_2-STZ

1 g of 3-chloropropyl trimethoxysilane-γ-Fe_2O_3/SiO_2) was mixed with 40 mL of ethanol and sonicated for 45 min. Subsequently, 1 g of sulfathiazole was added under mechanical stirring and the mixture was heated up to 80 °C for 24 h. Afterwards, the obtained solid was collected using a magnet, washed with diethyl ether (3 × 20 mL) and dichloromethane (3 × 20 mL) and dried at room temperature for 24 h.

3.5. Materials Characterization

The obtained nanomaterial was fully characterized by several techniques, including X-ray diffraction (XRD) analysis, N_2 adsorption-desorption measurements, energy-dispersive X-ray (EDX) analysis and scanning electron microscopy (SEM), pyridine (PY) and 2,6-dimethylpyridine (DMPY) titration, a vibrating sample magnetometer (VSM) study, and thermogravimetric analysis (TGA).

XRD analysis was performed in the Bruker D8 Advance Diffractometer with the LynxEye detector (Bruker AXS, Billerica, Massachusetts, USA). The XRD patterns were recorded in a 2θ scan range from 10° to 80°. Bruker Diffrac-plus Eva software, supported by Power Diffraction File database, was used for phase identification. In addition, SEM–EDX images were acquired in the JEOL-SEM JSM-7800 LV scanning microscope (JEOL, Dearborn Rd, Peabody, USA). TGA analysis was performed on a Perkin-Elmer thermal analyzer (Perkin-Elmer, Madrid, Spain), by heating the sample up to 800 °C at 10 °C min^{-1} under nitrogen atmosphere.

Pyridine (PY) and 2,6-dimethylpyridine (DMPY) titration experiments were carried out at 300 °C, via gas phase adsorption of the basic probe molecules applying a pulse chromatographic titration methodology. The catalyst (≈0.025 g) was fixed inside a tubular stainless steel microreactor (4 mm internal diameter) by Pyrex glass wool. A cyclohexane solution of titrant (0.989 M in PY and 0.686 M in DMPY, respectively) was injected into a gas chromatograph through the microreactor. The injected base was analyzed by gas chromatography with a flame ionization detector and using an analytical column of 0.5 m length, containing 5 wt% of polyphenylether in the Chromosorb AW-DMCS in 80/100. VSM study was performed by using the vibrating sample magnetometer (VSM)-LAKESHORE (Model: 7404, Lake Shore Cryotronics, Westerville OH, USA).

3.6. General Procedure for the Oxidation of Benzyl Alcohol to Benzaldehyde

Benzyl alcohol (0.1 mL, 1 mmol), γ-Fe_2O_3/SiO_2-STZ (25 mg) as catalyst, and acetonitrile (4 mL) as solvent were added into a necked flask and then H_2O_2 (50 wt%, 0.2 mL, 4 mmol) as oxidant agent was slowly dropped under stirrer and reflux conditions. The reaction mixture was kept at 80 °C and its progress was monitored by gas chromatography (GC) with a flame ionization detector (FID)

(AgilentTechnologies, GC6890N, (Agilent, Santa Clara, California, USA). The conversion and selectivity values were calculated as follows: (Equations (1) and (2))

$$\text{Conversion } (\%) = \left[\frac{C_{initial} - C_{final}}{C_{initial}}\right] \quad (1)$$

$$\text{Selectivity } (\%) = \frac{C_{product}}{[C_{initial} - C_{final}]} \times 100 \quad (2)$$

where $C_{initial}$ and C_{final} are the concentrations of reactant before and after the reaction, respectively, and $C_{product}$ is the concentration of product, as determined by gas chromatography.

3.7. General Procedure for the Alkylation Reaction of Toluene with Benzyl Chloride

Catalytic alkylation of toluene (2 mL) with benzyl chloride (0.2 mL) was performed using 25 mg of catalyst. The reaction was carried out assisted by microwave irradiation using the standard "open vessel" method (300 W, CEM-DISCOVER) at 90–100 °C for 3 min. Finally the reaction mixture was cooled down and filtered for further chromatographic analysis.

4. Conclusions

The successful synthesis of a sulfathiazole-modified γ-Fe_2O_3/SiO_2 core-shell nanoarchitecture was achieved by a multistep strategy. The γ-Fe_2O_3/SiO_2-STZ obtained exhibited interesting acid and magnetic features, which make it a potential candidate for its use in catalysis. Therefore, the catalytic performance of the prepared material was investigated in oxidation and alkylation reactions. In particular, γ-Fe_2O_3/SiO_2-STZ showed 95% of conversion and 97% of selectivity in the oxidation of benzyl alcohol to benzaldehyde, while it displayed conversion values higher than 99% in the alkylation of toluene with benzyl chloride. The magnetic properties of the catalyst allowed its simple recovery and reuse without a considerable loss of activity.

Supplementary Materials: The following are available online at https://www.mdpi.com/2073-4344/9/4/348/s1: Scheme S1: Illustration of the proposed mechanism for the oxidation reaction, Scheme S2: Proposed mechanism of the alkylation reaction; Figure S1: FT-IR spectra of the prepared materials of A) Sulfathiazole (STZ), B) γ-Fe_2O_3, C) γ-Fe_2O_3/SiO_2, and D) γ-Fe_2O_3/SiO_2-STZ.

Author Contributions: Data curation, D.R.-P.; Formal analysis, F.S.; Funding acquisition, R.L.; Investigation, S.O. and F.S.; Project administration, A.M.B. and R.L.; Resources, A.M.B. and R.L.; Supervision, D.R.-P. and A.M.B.; Validation, D.R.-P. and R.L.; Writing–original draft, S.O. and D.R.-P.; Writing–review and editing, A.M.B. and R.L.

Funding: This research was funded by MINECO, Spain, grant number CTQ2016-78289-P.

Acknowledgments: RL gratefully acknowledges MINECO as well as FEDER funds for funding under project CTQ2016-78289-P and financial support from the University of Cordoba (Spain). Daily Rodriguez-Padron also gratefully acknowledge MINECO for providing a research contract under the same project. The publication has been prepared with support from RUDN University Program 5-100.

Conflicts of Interest: The authors declare no conflict of interest.

References

1. Zeng, T.; Chen, W.W.; Cirtiu, C.M.; Moores, A.; Song, G.; Li, C.J. Fe_3O_4 nanoparticles: A robust and magnetically recoverable catalyst for three-component coupling of aldehyde, alkyne and amine. *Green Chem.* **2010**, *12*, 570–573. [CrossRef]
2. Zhu, Y.; Stubbs, L.P.; Ho, F.; Liu, R.; Ship, C.P.; Maguire, J.A.; Hosmane, N.S. Magnetic nanocomposites: A new perspective in catalysis. *ChemCatChem* **2010**, *2*, 365–374. [CrossRef]
3. Amali, A.J.; Rana, R.K. Stabilisation of Pd (0) on surface functionalised Fe_3O_4 nanoparticles: Magnetically recoverable and stable recyclable catalyst for hydrogenation and Suzuki–Miyaura reactions. *Green Chem.* **2009**, *11*, 1781–1786. [CrossRef]

4. Wu, L.; Tian, S. Immobilization of 1, 5, 7-Triazabicyclo [4.4.0] dec-5-ene on Magnetic γ-Fe_2O_3 Nanoparticles: A Highly Recyclable and Efficient Nanocatalyst for the Synthesis of Organic Carbonates. *Eur. J. Inorg. Chem.* **2014**, *2014*, 2080–2087. [CrossRef]
5. Xu, P.; Zeng, G.M.; Huang, D.L.; Feng, C.L.; Hu, S.; Zhao, M.H.; Cui, L.; Wei, Z.; Huang, C.; Xie, G.X.; et al. Use of iron oxide nanomaterials in wastewater treatment: A review. *Sci. Total Environ.* **2012**, *424*, 1–10. [CrossRef] [PubMed]
6. Rajabi, F.; Karimi, N.; Saidi, M.R.; Primo, A.; Varma, R.S.; Luque, R. Unprecedented selective oxidation of styrene derivatives using a supported iron oxide nanocatalyst in aqueous medium. *Adv. Synth. Catal.* **2012**, *354*, 1707–1711. [CrossRef]
7. Kitamura, H.; Zhao, L.; Hang, B.T.; Okada, S.; Yamaki, J.I. Effect of binder materials on cycling performance of Fe_2O_3 electrodes in alkaline solution. *J. Power Sources* **2012**, *208*, 391–396. [CrossRef]
8. Figuerola, A.; Di Corato, R.; Manna, L.; Pellegrino, T. From iron oxide nanoparticles towards advanced iron-based inorganic materials designed for biomedical applications. *Pharmacol. Res.* **2010**, *62*, 126–143. [CrossRef] [PubMed]
9. Deng, H.; Li, X.; Peng, Q.; Wang, X.; Chen, J.; Li, Y. Monodisperse magnetic single-crystal ferrite microspheres. *Angew. Chem. Int. Ed.* **2005**, *117*, 2842–2845. [CrossRef]
10. Wei, S.; Wang, Q.; Zhu, J.; Sun, L.; Lin, H.; Guo, Z. Multifunctional composite core–shell nanoparticles. *Nanoscale* **2011**, *3*, 4474–4502. [CrossRef]
11. Shylesh, S.; Schünemann, V.; Thiel, W.R. Magnetically separable nanocatalysts: Bridges between homogeneous and heterogeneous catalysis. *Angew. Chem. Int. Ed.* **2010**, *49*, 3428–3459. [CrossRef]
12. Ostovar, S.; Prinsen, P.; Yepez, A.; Shaterian, H.R.; Luque, R. Catalytic Versatility of Novel Sulfonamide Functionalized Magnetic Composites. *ACS Sustain. Chem. Eng.* **2018**, *6*, 4586–4593. [CrossRef]
13. Richter, M.K.; Sander, M.; Krauss, M.; Christl, I.; Dahinden, M.G.; Schneider, M.K.; Schwarzenbach, R.P. Cation binding of antimicrobial sulfathiazole to leonardite humic acid. *Environ. Sci. Technol.* **2009**, *43*, 6632–6638. [CrossRef] [PubMed]
14. Rahman, S.; Khan, R. Environmental pharmacology: A new discipline. *Indian J. Pharmacol.* **2006**, *38*. [CrossRef]
15. Cao, Q.; Dornan, L.M.; Rogan, L.; Hughes, N.L.; Muldoon, M.J. Aerobic oxidation catalysis with stable radicals. *Chem. Commun.* **2014**, *50*, 4524–4543. [CrossRef] [PubMed]
16. Abdallah, N.H. Immobilisation of Catalysts for Applications in Organic Reactions. Ph.D. Thesis, University of Limerick, Limerick, Ireland, 2016.
17. Rodríguez-Padrón, D.; Balu, A.M.; Romero, A.A.; Luque, R. New bio-nanocomposites based on iron oxides and polysaccharides applied to oxidation and alkylation reactions. *Beilstein J. Org. Chem.* **2017**, *13*, 1982–1993. [CrossRef]
18. Abednatanzi, S.; Abbasi, A.; Masteri-Farahani, M. Immobilization of catalytically active polyoxotungstate into ionic liquid-modified MIL-100 (Fe): A recyclable catalyst for selective oxidation of benzyl alcohol. *Catal. Commun.* **2017**, *96*, 6–10. [CrossRef]
19. Ryland, B.L.; Stahl, S.S. Practical aerobic oxidations of alcohols and amines with homogeneous copper/TEMPO and related catalyst systems. *Angew. Chem. Int. Ed.* **2014**, *53*, 8824–8838. [CrossRef]
20. Reddy, C.; Reddy, S.R.; Naidu, S. Chemoselective Oxidation of Benzyl, Amino, and Propargyl Alcohols to Aldehydes and Ketones under Mild Reaction Conditions. *ChemistryOpen* **2015**, *4*, 107–110. [CrossRef] [PubMed]
21. Meng, C.; Yang, K.; Fu, X.; Yuan, R. Photocatalytic oxidation of benzyl alcohol by homogeneous $CuCl_2$/solvent: A model system to explore the role of molecular oxygen. *ACS Catal.* **2015**, *5*, 3760–3766. [CrossRef]
22. Prebil, R.; Stavber, G.; Stavber, S. Aerobic Oxidation of Alcohols by Using a Completely Metal-Free Catalytic System. *Eur. J. Org. Chem.* **2014**, *2014*, 395–402. [CrossRef]
23. Verma, S.; Baig, R.N.; Nadagouda, M.N.; Varma, R.S. Selective oxidation of alcohols using photoactive VO@ g-C_3N_4. *ACS Sustain. Chem. Eng.* **2016**, *4*, 1094–1098. [CrossRef]
24. Hosseinpour, R.; Pineda, A.; Ojeda, M.; Garcia, A.; Romero, A.A.; Luque, R. Microwave-assisted oxidation of benzyl alcohols using supported cobalt based nanomaterials under mild reaction conditions. *Green Process. Synth.* **2014**, *3*, 133–139. [CrossRef]
25. Hyeon, T.; Lee, S.S.; Park, J.; Chung, Y.; Na, H.B. Synthesis of highly crystalline and monodisperse maghemite nanocrystallites without a size-selection process. *J. Am. Chem. Soc.* **2001**, *123*, 12798–12801. [CrossRef]

26. Yepez, A.; Hidalgo, J.M.; Pineda, A.; Černý, R.; Jíša, P.; Garcia, A.; Luque, R. Mechanistic insights into the hydroconversion of cinnamaldehyde using mechanochemically-synthesized Pd/Al-SBA-15 catalysts. *Green Chem.* **2015**, *17*, 565–572. [CrossRef]
27. Luque, R.; Campelo, J.M.; Luna, D.; Marinas, J.M.; Romero, A.A. NH_4F effect in post-synthesis treatment of Al-MCM-41 mesoporous materials. *Microporous Mesoporous Mater.* **2005**, *84*, 11–20. [CrossRef]
28. Rajpure, K.Y. Exploring structural and magnetic properties of nanocrystalline iron oxide synthesized by autocombustion method. *Superlattices Microstruct.* **2015**, *77*, 181–195. [CrossRef]
29. Cheon, J.; Kang, N.J.; Lee, S.M.; Lee, J.H.; Yoon, J.H.; Oh, S.J. Shape evolution of single-crystalline iron oxide nanocrystals. *J. Am. Chem. Soc.* **2004**, *126*, 1950–1951. [CrossRef]
30. Shi, J.; Ai, Z.; Zhang, L. Fe@ Fe_2O_3 core-shell nanowires enhanced Fenton oxidation by accelerating the Fe (III)/Fe (II) cycles. *Water Res.* **2014**, *59*, 145–153. [CrossRef]
31. Xiao, S.; Zhang, C.; Chen, R.; Chen, F. Selective oxidation of benzyl alcohol to benzaldehyde with H_2O_2 in water on epichlorohydrin-modified Fe_3O_4 microspheres. *New J. Chem.* **2015**, *39*, 4924–4932. [CrossRef]
32. Bachari, K.; Millet, J.M.M.; Benaıchouba, B.; Cherifi, O.; Figueras, F. Benzylation of benzene by benzyl chloride over iron mesoporous molecular sieves materials. *J. Catal.* **2004**, *221*, 55–61. [CrossRef]
33. Kalita, P.; Gupta, N.M.; Kumar, R. Synergistic role of acid sites in the Ce-enhanced activity of mesoporous Ce–Al-MCM-41 catalysts in alkylation reactions: FTIR and TPD-ammonia studies. *J. Catal.* **2007**, *245*, 338–347. [CrossRef]
34. Gracia, M.J.; Losada, E.; Luque, R.; Campelo, J.M.; Luna, D.; Marinas, J.M.; Romero, A.A. Activity of Gallium and Aluminum SBA-15 materials in the Friedel–Crafts alkylation of toluene with benzyl chloride and benzyl alcohol. *Appl. Catal. A General* **2008**, *349*, 148–155. [CrossRef]
35. Ziarati, A.; Badiei, A.; Luque, R.; Ouyang, W. Designer hydrogenated wrinkled yolk@ shell TiO_2 architectures towards advanced visible light photocatalysts for selective alcohol oxidation. *J. Mater. Chem. A* **2018**, *6*, 8962–8968. [CrossRef]



© 2019 by the authors. Licensee MDPI, Basel, Switzerland. This article is an open access article distributed under the terms and conditions of the Creative Commons Attribution (CC BY) license (http://creativecommons.org/licenses/by/4.0/).